POAC'13
Espoo, Finland

Proceedings of the 22nd International Conference on
Port and Ocean Engineering under Arctic Conditions
June 9-13, 2013
Espoo, Finland

Buried Pipeline Response to Ice Gouging on a Clay Seabed Large Scale Tests and Finite Element Analysis

Ralf Peek[1], Ken Been[2], Vincent Bouwman[1], Arash Nobahar[3], Rodolfo Sancio[4], Ruben van Schalkwijk[5]
[1]Shell Global Solutions, Rijswijk, The Netherlands
[2]Golder Associates, Halifax, Canada
[3]Shell, Houston, Texas
[4]MMI Engineering, Houston, Texas
[5]RVS Engineering, Huizen, The Netherlands

ABSTRACT

An ice gouge on the seafloor transmits loads to a buried pipeline via the soil, even if the burial depth is greater than the gouge depth. To validate finite element models that capture this, tests have been carried out at as large a scale as practical, using rigid indenters as ice keels. This papers covers tests performed in clay including a buried steel pipe, finite element (FE) modelling thereof, using a fully coupled model based on an Eulerian representation of the soil, and a Lagrangian representation of the keel and the pipe.

For the FE model, undrained conditions are assumed, and the total stress response of the clay determined using a time-invariant elastoplastic material based on the Von Mises yield surface with isotropic strain hardening, and the stress-strain curve obtained from unconfined compression (UC) tests.

Despite the simplicity of the soil modelling, the FE results for strains in a buried steel pipe are in agreement with the values from the test. Subgouge deformations away from the pipe from the FE analysis are small, but those from the test even smaller. This paper provides further details of the tests, the FE analysis and the comparison of results for gouge depth, pulling force, subgouge deformations and pipe response.

INTRODUCTION

Where the seafloor is subject to ice gouges from ice keels formed of frozen seawater, subsea pipelines must not only be protected from direct impact by such an ice keel, but the pipe must also withstand loads and displacements transmitted to it via the soil between the keel and the pipeline. This paper addresses the pipe response under such indirect ice loads. If the pipeline offered no resistance to movements, the displacements imposed on it would be the subgouge displacements, which are defined as the soil displacements under the gouge in absence of the pipeline. Due to pipe stiffness, the pipe undergoes smaller displacements. To determine how much smaller and the pipe deformation, ice-soil-pipe interaction must be considered.

Here a coupled finite element (FE) model is used in which the soil is modelled as a three-dimensional continuum with Eulerian elements. The FE results are compared with results from two physical tests involving a compacted clayey soil. The tests are labelled "Test 7" and "Test 8" with key test parameters given in Table 1. They are carried out at as large a scale as practical, by towing rigid "keels" (made of steel and concrete) over the prepared soil and a buried pipeline with a bulldozer (Sancio et al. 2011), as shown in Fig. 1.

Coupled finite element (FE) models of the gouging process are not new [Kenny et al. (2005), Konuk et al. (2005a,b, 2006), Nobahar et al. (2007), Lele et al. (2011), Peek and Nobahar (2012)], nor are tests [Poorooshasb et al. (1989), Lach (1996), Phillips et al. (2005), Been et al. (2008)]. However, to the author's knowledge this is the first time gouging tests with a pipe have been done at such a large (though still not full) scale, together with detailed FE to verify the ability of the FE model to capture the essence of the phenomena involved.

Figure 1. Typical gouging test in clay using a rigid indenter as "ice keel".

SOIL PROPERTIES AND FINITE ELEMENT (FE) MODELING THEREOF

The gouging tests were performed in Texas using a compacted a soil chosen to reproduce approximately typical conditions at the Kashagan field in the North Caspian, Republic of Kazakhstan. For this purpose, the soil had about 45% of fine-grained particles (i.e., < 0.075 mm), and about 28% clay-sized particles (i.e., < 0.002 mm). The liquid limit of the material ranged between 35 and 40 and the plastic limit between 13 and 15. The soil therefore classified as clayey sand (SC) according to the USCS. However, the mechanical response of the material resembled the typical mechanical response of clay. The clayey sand is referred to as "clay".

The clay was moisture conditioned in a specially designated area of the test site where a layer of excavated clay clods was laid. The large clods of clay were then broken into smaller clods using a rototiller. Water was then added with a rear sprayer. The moist clay was subsequently tilled once again with the rototiller and repeatedly mixed by pushing it into windrows using a motor grader. This reduced the diameter of the clods to 2cm or less. A nuclear densometer was used to monitor the water content. This clay was then compacted with a Hamm 3410 smooth drum roller in lifts of about 10 to 30 cm in thickness.

Although this method did not produce a fully saturated soil, the soil was modelled as clay under undrained conditions. This was further approximated as an elastic-plastic material

yielding according to the Von Mises yield criterion with isotropic strain hardening, and stress-strain curves calibrated to more or less match those for the soil under unconfined compression (UC) tests, as shown in Figs. 2. (The elastic-plastic Von Mises material represents the total stress response of the saturated clay under undrained conditions.) The variability in strength from the UC tests in Fig. 2, is typical of the variability encountered from various methods of measuring or estimating the strength, which included torvane tests, and strength estimated from the water content and a correlation to strengths from specimen compacted in the laboratory, as well as the UC tests on samples compacted in the field. It is thought that this largely represents actual variability in soil properties "as compacted" in the test bed, e.g. due to desiccation although the use of desiccated parts of stockpiled clay was avoided.

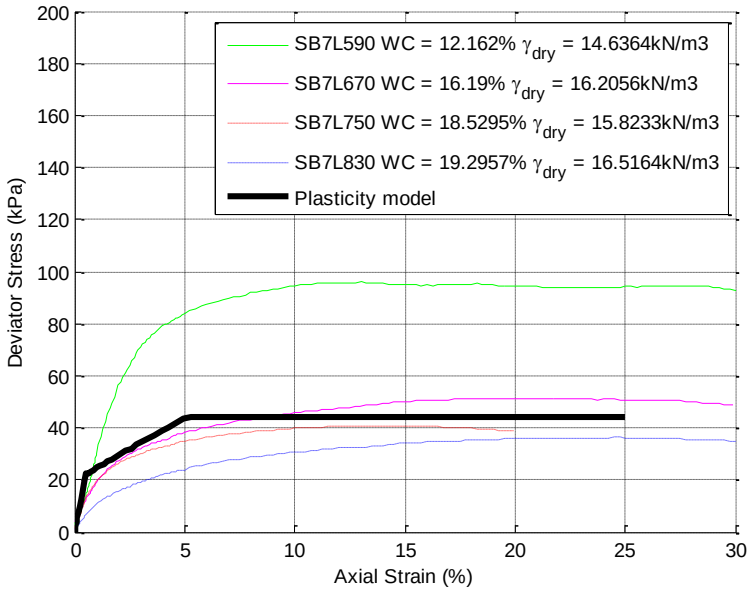

Figure 2a. Stress-strain curves from unconfined compression (UC) tests on the clay compared with the stress-strain curve used in the modelling of the tests (shown in black), for Test 7.

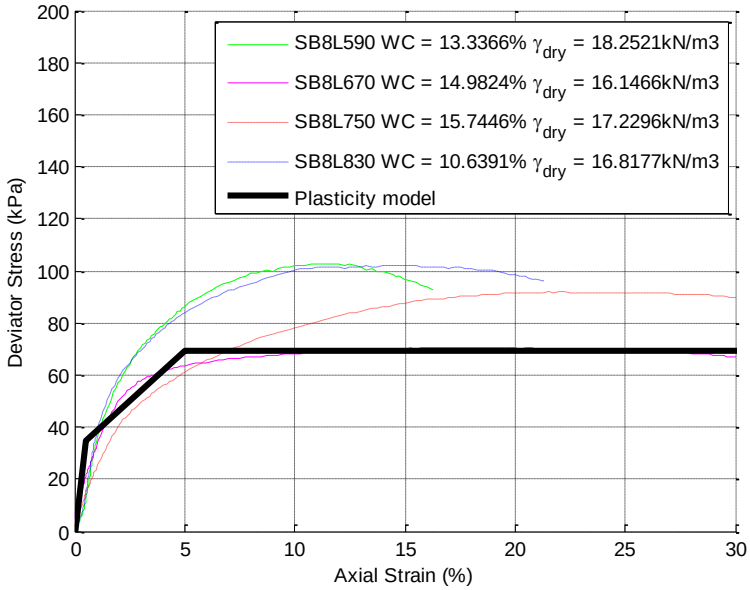

Figure 2b. Stress-strain curves from unconfined compression (UC) tests on the clay compared with the stress-strain curve used in the modelling of the tests, for Test 8.

Table 1. Key Test Parameters and Soil Properties Used in FE Analysis

Test Identification	Test 7	Test 8
Keel Width	2.44 m	1.60 m
Keel Weight	557 kN	453 kN
Approximate gouge depth reached (this is a result of the test, since the keel was free to move up or down and to rotate until a roughly steady-state equilibrium was reached)	0.9 m	0.6 m
Pipeline Outer Diameter	The keel did not reach the pipeline.	168.3 mm
Pipeline Wall Thickness		11 mm
Burial depth to Top of Pipe		0.85 m
Undrained Shear Strength of the Clay	25.5 kPa	40 kPa
Young's modulus of the Clay	4420 kPa	6920 kPa
Poisson's ratio	0.4	
Soil Unit Weight	19 kN/m^3	19.5 kN/m^3
Keel-soil and pipe-soil interface shear strength coefficient (shear strength of interface divided by that of the soil) [American Lifelines Alliance (2001)]	$\alpha = 0.93$	$\alpha = 0.78$

The mathematical soil used in the FE (finite element) analysis has tension as well as compression capacity. If conditions in saturated clay were truly undrained, it too would have tension capacity, at least until cavitation of the pore water. However it is known [Rice (1975)] that deformations in saturated materials tend to localize with local drainage, resulting in loss of tension capacity when yielding under tension. This aspect is not captured by the FE model, however. It plays a significant role in the soil berms that are thrown up by the gouging process, where the clay is seen to break up into lumps.

DESCRIPTION OF THE TESTS

The test clay was compacted into an excavated test basin of trapezoidal cross section, 1.8 m deep, and 4 m wide at the base. The geometry and dimensions of the keels are shown in Fig. 3. These keels are pulled along the test basins with the bulldozer, with a pull cable attached to the end of the yoke.

Both tests included a buried pipeline with end plates to simulate the axial restraint that would arise for a very long pipeline. However, for Test 7, the keel got stuck before reaching the pipeline, due to a high build-up of the berm in front of the keel. Therefore pipe strains are given only for Test 8. The pipe is buried to a depth of 0.85 m to the top of the pipe. It is placed in a trench and backfilled with clay compacted to about the same properties as the soil outside this trench.

Subgouge displacements were measured by placing markers at a location not affected by the pipeline. The location of the markers is surveyed when placed, in between lifts of compacted soil, and again upon careful excavation after the test, so that subgouge displacements could be determined as the difference in marker positions.

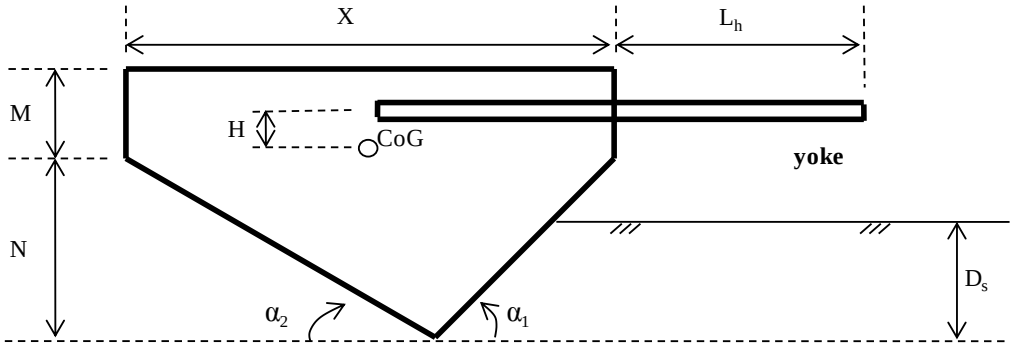

	Keel #2 (Clay Test #7)	Keel #1 (Clay Test #8)
Width [m]	2.44	1.60
Weight [kN]	557	453
L_h [m]	3.00	3.00
M [m]	0.94	0.94
N [m]	1.30	1.50
H [m]	-0.10	-0.04
X [m]	5.82	6.71
α_1 [degrees]	30	30
α_2 [degrees]	20	20

Figure 3. Geometry and dimensions of the keels.

DESCRIPTION OF THE FINITE ELEMENT (FE) MODEL

The FE analyses are done with the Abaqus/Explicit version 6.9-EF program. Eulerian elements are used for the soil, while the ice and the pipe models are Lagrangian. The Eulerian and Lagrangian elements interact by the "CEL" (Coupled Eulerian-Lagrangian) feature of Abaqus. This originates from modelling fluid-structure interaction problems, except that in this case the fluid is replaced by the Eulerian soil domain. The Eulerian mesh is fixed in space and must cover the all the space that might be occupied by soil at any time during the test. Elements in the Eulerian mesh can fill and empty with soil, as soil-air, soil-pipe, or soil-keel boundaries move across them. The advantage of the Eulerian formulation for the soil is that the mesh does not distort with the soil, and thus very large soil deformations are possible without the mesh becoming hopelessly distorted.

The pipe is modelled with beam elements together with Lagrangian solid elements that are very soft compared to the pipe, yet stiff compared to the soil. These elements are referred to here as load-transfer elements. They can transfer the loads from the soil to the pipe even though the beam elements are just lines with zero cross sectional dimensions. (The cross sectional dimensions are used by the beam elements only to determine the stiffness and strength of the line.) Compared to the alternative of using shell elements to model the pipe, this approach allows the use of larger elements for steel. Thereby a larger time increment is possible in the explicit time-integration without loss of stability. The load-transfer elements are elastic with a modulus of elasticity of 1GPa, which is more than 100 times that of the soil and less than 1% of that of the pipe. The flexural stiffness of the load-transfer elements is about 0.8% of that of the pipe in the elastic condition. On this basis the load-transfer

elements are expected to work as intended while the pipe remains elastic, as it does for the analyses reported here. For further validation of the load-transfer-elements approach a smaller test problem was used, involving pushing a sphere into the soil near the pipe. For this an Eulerian model with load-transfer elements gave similar responses as a Lagrangian FEA model without load-transfer elements.

Symmetry about the centre plane of the gouge is exploited in the FE model.

The shear strength at the keel-soil and pipe-soil interfaces are determined a factor α times the soil shear strength, or 3 times the normal stress, whichever is less. This way it is possible to capture loss of contact without tension being developed, while at the same time reaching the desired interface shear strength at low values of the normal force. The values of α used are determined from [American Lifelines Alliance (2001)].

In the model the keel is first pushed into the soil, and then pulled from the yoke until a more or less steady-state gouging condition develops, that does not depend on how the keel was initially pushed into the soil. Conditions of the soil at the end of a FE run are shown in Fig. 4.

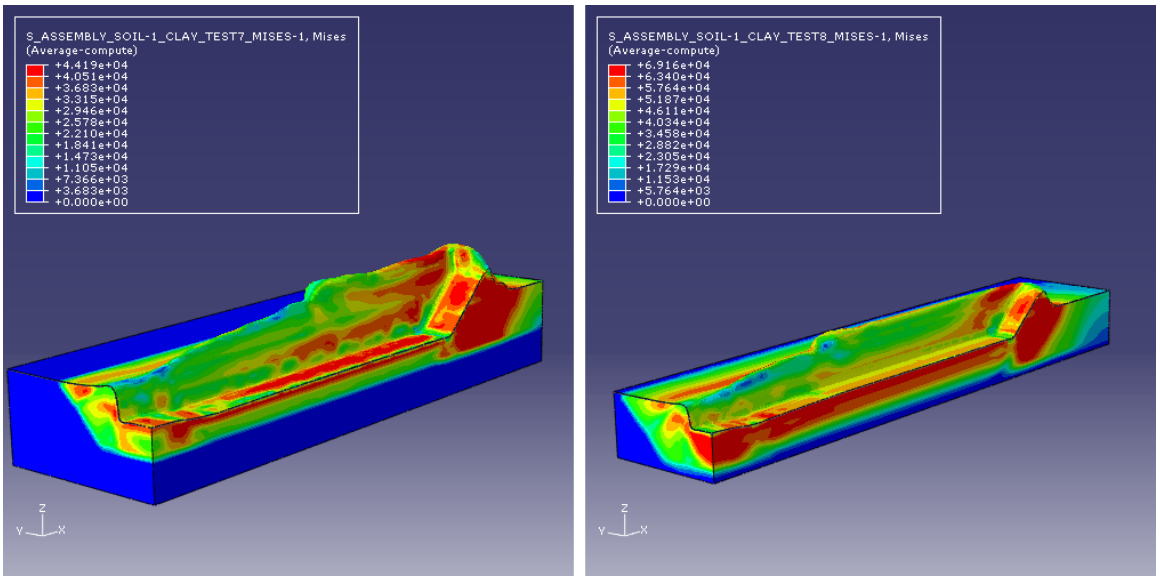

Figure 4. Gouge and berm geometry for Test 7 (left) and Test 8 (right). Colors represent the Von Mises equivalent to the axial stress in a UC test, which reaches a maximum value on the flat portion of the stress-strain curve in Fig. 2 of 44.2kPa for Test 7, and 69.2kPa for test 8, corresponding to √3 times the undrained shear strength.

RESULTS

The keel is free to move up or down under its weight or to rotate, eventually a roughly steady-state equilibrium gouge depth is reached, as shown in Fig. 5. The FE gouge depth quickly reaches a steady state, which is more or less in agreement with the gouge depths reached during the tests. The exact reason for changes in depth in the tests is unclear, but the variability in soil properties shown in Fig. 2 could contribute to this.

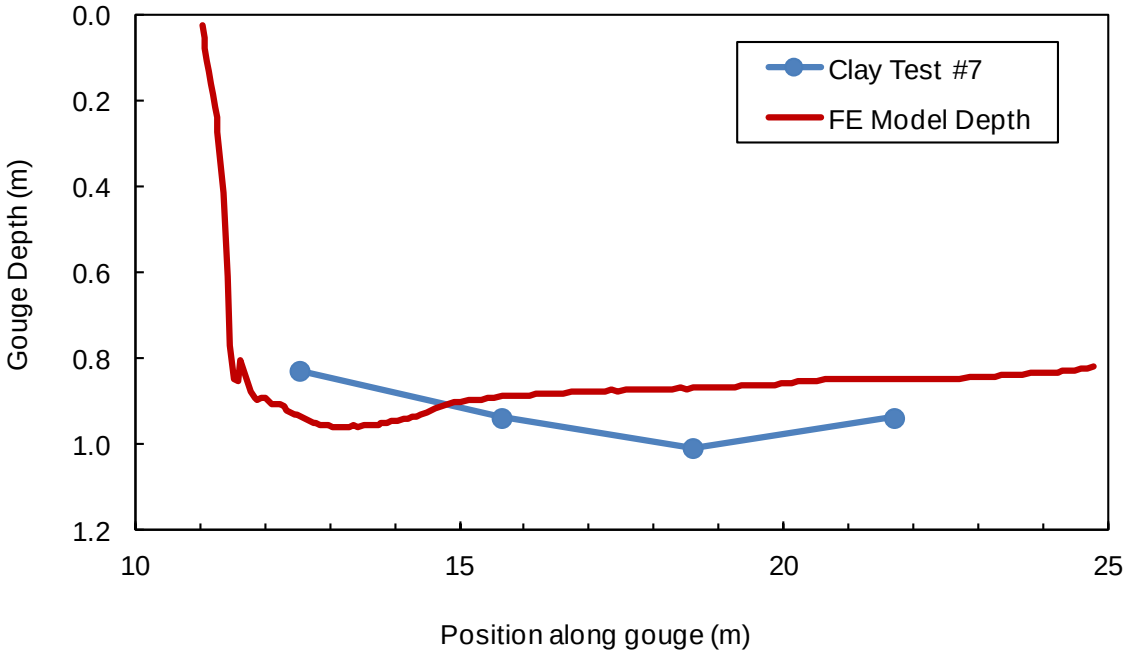

Figure 5a. FE analysis vs. test comparison of gouge depths as a function of position along the gouge for Test 7.

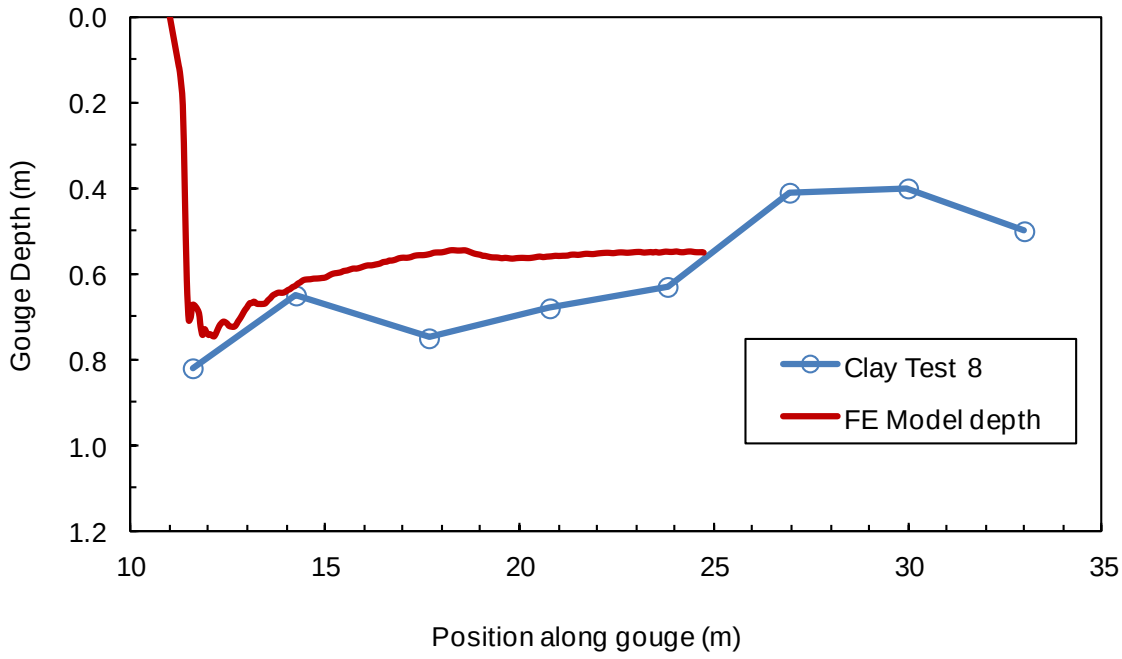

Figure 5b. FE analysis vs. test comparison of gouge depths for Test 8.

The pulling forces from the FE analyses are also more or less in agreement with those from the tests, with the latter being more variable and peaks up to 50% or so higher, perhaps in part due to strain rate effects on the soil, which were not considered. The FE model strengths are calibrated based on the lower strain rate of the laboratory UC tests.

Subgouge displacements of markers at different depths below the keel in the tests are shown on Fig. 6. For comparison with the FE analysis, points initially at an elevation of about 0.1m

below that of the bottom of the keel during gouging are shown in Fig. 7. It is clear that the subgouge deformations from the tests are very small, whereas the FE analysis shows considerable subgouge deformations at this depth. It is possible that this is merely a mesh effect. To get accurate displacements at only 0.1m below the bottom of the keel, the element size there would have to be much smaller than 0.1m. The actual size of the elements there is about 0.08m, with linear interpolation between nodes at the corners of distorted-brick-shaped elements. In addition to mesh effects near surfaces of discontinuous velocity of the soil, the modelling of the stress-strain curve of the soil can also have a significant influence on subgouge deformations. Parametric studies indicate that where more deformation is needed to develop the strength of the soil, larger subgouge deformations are calculated. Choosing the stress-strain curves to match the soil response in simple shear or extension could thus lead to different results from those calculated using the stress-strain curves from unconfined compression (UC) tests.

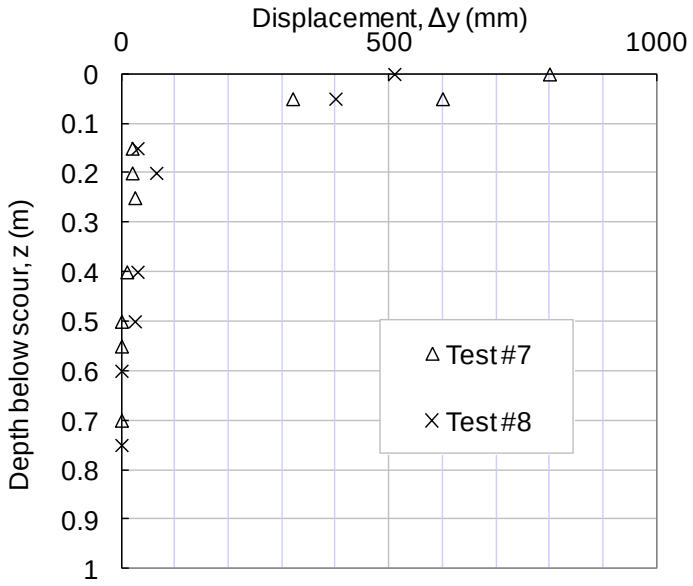

Figure 6. Horizontal component of subgouge displacement as a function of depth below keel at the centre plane of the gouge.

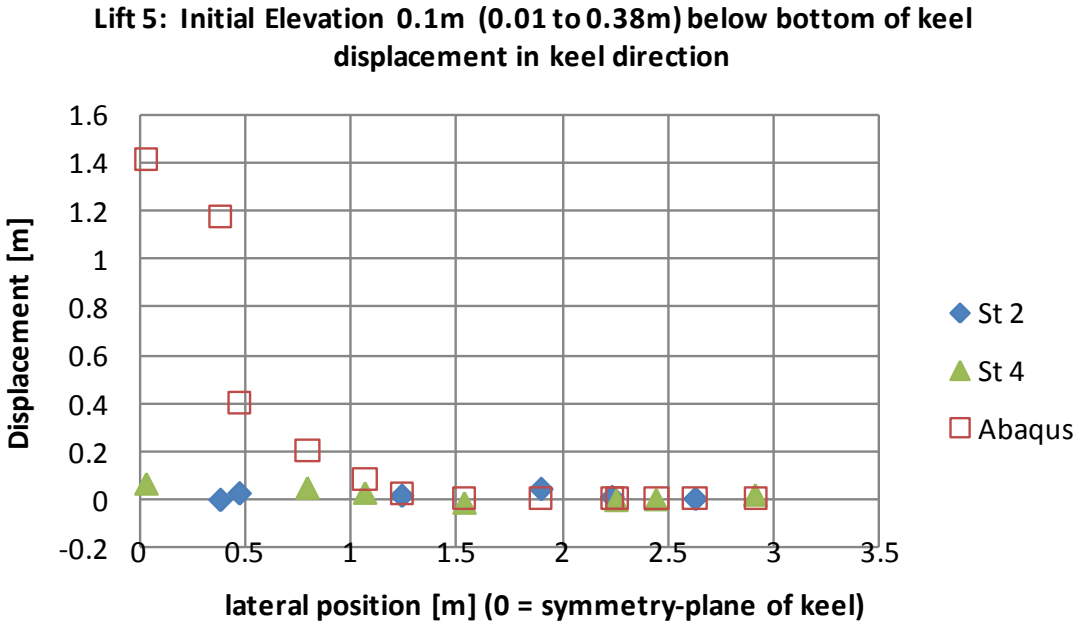

Figure 7. FE vs. Test 8 comparison of subgouge displacements (magnitude of vector) of points initially at an elevation of about 0.1m below the keel for Test 8, shown as a function of distance from the plane of symmetry.

The strains in the buried pipe for Test 8 are shown in Fig. 8. It is clear that the strains are very small, and at least the component due to horizontal bending is surprisingly accurately matched by the FE analysis. The ends of the pipe are at about x=6.25m from the plane of symmetry, the pipe is assumed to be fully fixed. Although this exaggerates the limited restraint provided by the end plates, it is not expected to affect the pipeline where the gouging takes place. (For heavier gouge loads and larger pipe deformations the end conditions do matter, because the gouging changes the axial force in the line, and this effect extends to a considerable distance from the gouge, but this is not the case for the very small deformations that occurred in this test.)

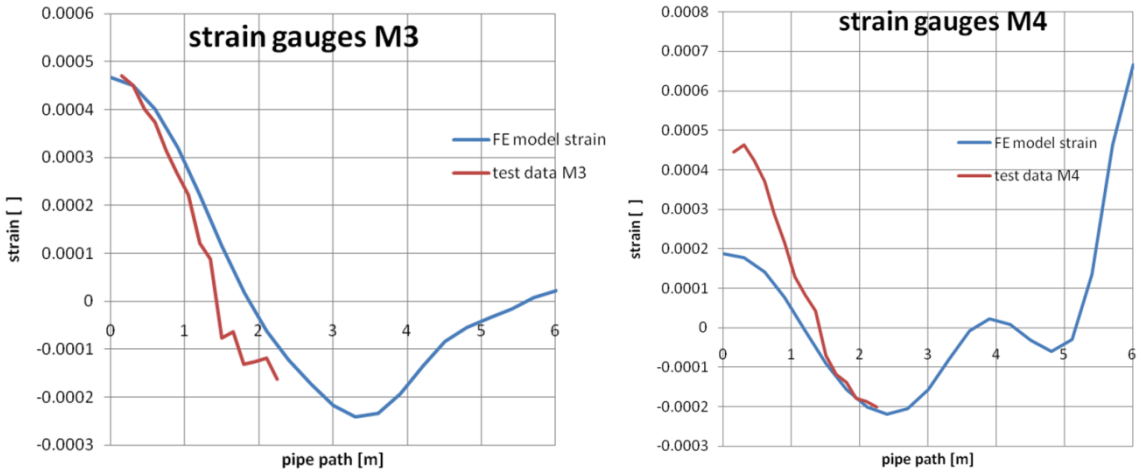

Figure 8. FE vs. Test 8 comparison of strains in the pipe due to horizontal bending (left) and vertical bending (right), shown as a function of the distance from the plane of symmetry

CONCLUSIONS

It is demonstrated that, at least for the example considered involving non-sensitive clay, Finite Element Analysis (FEA) calibrated based on (small scale) laboratory tests on soil samples can reproduce the effect of gouging the seafloor with a rigid indenter on a buried pipe. The test results for the strains in a buried pipe, the force required to pull the indenter, and the gouge depth for a given weight of the indenter are reproduced within the accuracy to which test parameters such as soil properties are controlled in the tests.

The tests did involve considerable point-to-point variations in soil properties, with a coefficient of variation in strength of around 30% (based on torvane tests), and a factor of around 3 difference between maximum and minimum soil shear strength (for both torvane and unconfined compression tests from field samples). This limits the accuracy to which FEA predictions could be verified. Possible reasons for the variable soil properties in the test include insufficient mixing of the soil and/or control of the water added, non-uniform desiccation of the soil , or heterogeneity of the sourced material.

The simple soil model used does not reproduce the disintegration of the clay into lumps in the berms produced by gouging. Air entrainment has taken place between such lumps perhaps starting at cracks or gaps that formed. This is contrary to the assumption of saturated continuum, undrained soil behaviour. The cracking and air entrainment prevent the development of tensile strength by pore water suction. As a result the FEA tends to predict berms that are too strong and grow too high without collapsing and flowing around the keel. Nevertheless this modelling error hardly seems to influence the effects of gouging on the

buried pipe, or any of the above-quoted parameters reproduced by the FE analysis. This may also be because the FE model spoil heap is narrower (as measured in the gouging direction), so that its weight is similar to that in the test. It is also conceivable that some of the FE berms heights had not quite reached steady-state.

ACKNOWLEDGEMENTS

The authors would like to thank the North Caspian Production Operations Company (NCPOC) and the Kashagan project partners for permission to publish this paper.

REFERENCES

Allersma, H.G.B., and Schoonbeek, I.S.S. (2005), Centrifuge modelling of scouring ice keels in clay. Int. Conference on Offshore and Polar Engineering, ISOPE2005, Seoul, June 19-24, paper 2005-JSC-427, pp.404-409.

American Lifelines Alliance (2001). Guidelines for the Design of Buried Steel Pipe. ASCE, 76 pages.

Been, K., et al., (2008), "Subscour Displacement from Physical Model Tests," 7th International Pipeline Conference, September 29–October 3, 2008, Calgary, Alberta, Canada, Paper No. IPC 2008-64186.

Kenny, S., Phillips, R., Clark, J. I., and Nobahar, A. (2005). "PRISE numerical studies on subgouge deformations and pipeline/soil interaction analysis." POAC, 43-52.

Konuk, I., Yu, S., and Garcia, R., (2005a), "An ALE FEM Model of Ice Scour," 11th International Conference of the International Association of Computer Models and Advances in Geomechanics, Turin, Italy, June, 2005.

Konuk, I., Yu, S., Gracie, R., (2005b), "A 3-Dimensional Continuum ALE Model for Ice Scour - Study of Trench Effects," Proc. 24th Int. Conf. on Offshore Mechanics and Arctic Engineering, 12-17 June 2005, Halkidiki, Greece, Paper No. OMAE2005-67547.

Konuk, I., Yu, S., and Fredj, A. (2006). "Do Winkler Models Work: A Case Study for Ice Scour Problem", OMAE, paper # 92335, Hamburg, Germany.

Lach, P.R. (1996), "Centrifuge Modelling of Large Soil Deformation due to Ice Scour," Doctoral Thesis, Memorial University of Newfoundland.

Lele, S.P., et al. (2011), "3D Continuum Simulations to Determine Pipeline Strain Demand due to Ice-Gouge Hazards," Arctic Technology Conference, Houston, Texas, USA, 7–9 February 2011, Paper No. OTC 22109.

Nobahar, A, Kenny, S., and Phillips, R. (2007). "Buried Pipelines Subject to Subgouge Deformations" Int. J. Geomech., ASCE, 7(3), 206–216.

Peek, R. and Nobahar, A. (2012). "Ice Gouging over a Buried Pipeline: Superposition Error of Simple Beam-and-Spring Models." Int. J. Geomech., ASCE, 12(4), 508–516.

Phillips, R., Clark, J. I., and Kenny, S., 2005. (2005). "PRISE studies on gouge forces and subgouge deformations." Proc. 18th POAC, 75-84.

Poorooshasb, F., Clark, J.I. and Woodworth-Lynas, C.M.T.,(1989) "Small scale modelling of iceberg scouring of the seabed". POAC Conference, p133-145.

Rice, J.R., (1975), "On the Stability of Dilatant Hardening for Saturated Rock Masses," Journal of Geophysical Research, Vol. 80, No. 11, pp. 1531-1536, April 10, 1975.

Sancio, R.B., Been, K. and Lopez, J., (2011) "Large Scale Indenter Test Program to Measure Sub Gouge Displacements," Proceedings of 21st International Conference on Ports and Ocean Engineering under Arctic Conditions, Montreal, Canada. POAC 11-96.